An Image Analysis System for the Assessment of Retinal Microcirculation in Hypertension and Its Clinical Evaluation

X. Zabulis[1], A. Triantafyllou[2], P. Karamaounas[1], C. Zamboulis[2], and S. Douma[2]

[1] Institute of Computer Science, Foundation for Research and Technology - Hellas
[2] 2nd Propaedeutic Dept. of Int. Medicine, Hippokration General Hospital,
Aristotle University of Thessaloniki, Thessaloniki, Greece

Abstract— **A system for the assessment of hypertension through the measurement of retinal vessels in fundoscopy images, is presented. The proposed approach employs multiple image analysis methods, in an integrated system that is used in clinical practice. Automating the measurement process enables the conduct of a clinical study that, for the first time, shows the correlation between macrovascular and microvascular alterations, based on numerous measurements acquired by this system. Experience and perspectives gained from clinical usage and evaluation are reported.**

I. Introduction

Cardiovascular disease is a leading cause of mortality and morbidity, with cardiovascular events accounting for about one-third of the recorded deaths worldwide [4]. Hypertension (high blood pressure) is one of the most important, highly prevalent and reversible cardiovascular risk factors and the World Health Organization has rated hypertension as one of the most important causes of premature death worldwide. Until recently, cardiovascular disease, which clinically manifests mainly as myocardial infarction and stroke, was considered to involve primarily large vessels. Recent research has highlighted the crucial involvement of the microcirculation in many cardiovascular conditions [15, 14]. The retina is an accessible "window" through which the microcirculation can be depicted directly and repeatedly through time [7]. As new assessment methods and software automation become widely available, abnormalities of microcirculatory function can be detected non-invasively and cost-efficiently through fundoscopy.

During the last years, automated vessel detection software provided the opportunity to investigate the clinical and prognostic significance of retinal vessel alterations, as well as the pathophysiological mechanisms linking them to hypertension and cardiovascular diseases. Thorough assessment of these alterations over time, during the course of the disease and after the administration of appropriate treatment is considered still inadequate. The lack of relevant software (able to match different images of the same patient, obtained at different time points) might explain why there are only a few studies, most of them with major methodological limitations, investigating whether the eligible anti-hypertensive treatment can reverse retinal alterations and reduce patient cardiovascular risk [17, 22].

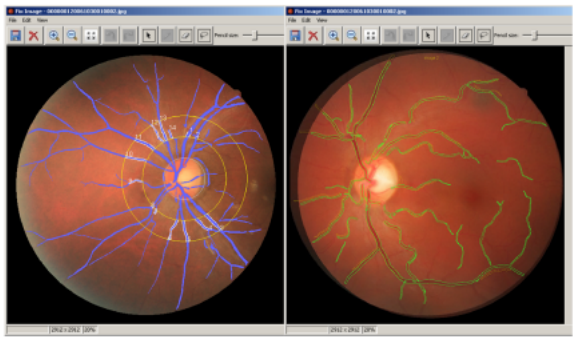

Fig. 1 User interface components for vessel measurement (left) and comparison of two registered diagnostic images, of the same patient (right).

The key measurement, in this work, is the width of vessels as it indicates a remodeling of vessel walls: as blood pressure rises vessel walls undergo a narrowing of the internal lumen and, in turn, vessel image width. Despite ongoing research in retinal image analysis (see [2] for a review), there is a disparity between current state-of-the-art and the software applications available to the healthcare professional. Currently, the clinical practitioner lacks tools that find vessels and measure them, in a highly usable and automatic manner. Furthermore, progress marked in vessel segmentation and width measurement, has not yet been matched by progress in monitoring patient status along time, so as to associate and compare measurements from different examinations, i.e. screening and follow-up.

In this work, we propose an image analysis system that extends state-of-the art in the automatic assessment of hypertensive signs in fundoscopy images. Fig. 1, shows two central panels of the proposed system. The left presents vessel detection and measurement around the detected optical disk for computation of a diagnostic metric called ArterioVenus Ratio (AVR). The right shows an image registration process that enables the comparison of measurements from different examinations, at the same anatomical locations. Besides

L.M. Roa Romero (ed.), *XIII Mediterranean Conference on Medical and Biological Engineering and Computing 2013,*
IFMBE Proceedings 41,
DOI: 10.1007/978-3-319-00846-2_82,

encapsulating state-of-the-art methods for image segmentation and measurement, the proposed system employs image analysis methods in the user interface, to increase usability in tasks such as the selection of vessels to measure and the comparison of their dimensions.

The remainder of this paper is organized as follows. In Sec. II related work is reviewed. In Sec. III the proposed system is presented and in, Sec. IV, the conducted clinical study is described. Clinical perspectives, system evaluation, and directions for future work are provided in Sec. V.

II. Related work

Simple fundoscopy modalities are accompanied by software that performs basic observation and file management functions, such as the "2D/3D Non-mydriatic Retinal Camera / Analysis System" (*Kowa Optimed*), the "DRS non-mydriatic fundus camera" (*CenterVue*), the "VISUCAM-PRO" (*Carl Zeiss Meditec*), and the "IMAGEnet" (*Topcon*).

More advanced systems perform "generic" image analysis in the sense that they detect anatomical features, such as blood vessels, the optic disc, and the fovea [6, 19]. Methods of such systems can be the basis for a wide-range of diagnostic studies, but their integration with additional context-based techniques is still required in clinical practice.

Despite the lack of systems for the detection of hypertensive signs in retinal images, progress has been made in the domain of diabetes. Pertinent applications are not directly relevant, but include functionalities useful for the assessment of retinal microcirculation in hypertensive patients. The "Diabetic Retinopathy Risk Analyzer" (*VisionQuest Biomedical*), provides automatic AVR computation and tools for artery-vein classification. "Retinal Analysis Tool" (*ADCIS*) includes semi-automatic tools for vessel segmentation but focuses on diabetic retinopathy and age-related macular degeneration. "SIRIUS" [12] is an online-system for lesion detection and AVR computation. "DR-CAD" [1] is a screening system for diabetes that uses machine learning to detect vessels, optic disk, and lesions.

Retinal image analysis systems that provide registration functionalities focus on the spatial domain. I.e. "DualAlign i2k Retina" (*Topcon Medical Systems*) and "AutoMontage" (*MediVision Medical Imaging*) stitch retinal images together to create a "montage": a composite image showing a larger region of the retina. However, there is lack of work in temporal image registration. The need, in this case, is to register two images of the same anatomical location, acquired over widely separated time instances (i.e. 6 months). The goal is to compare changes, due to the manifestation of a disease or the reversal of symptoms due to the administered treatment.

Our work in [10] was evaluated on benchmark datasets to provide state-of-the-art accuracy in vessel segmentation. In *this work*, we capitalize on this accuracy in the context of a clinical study, to capture variations in vessel width and AVR values that are linked to hypertension. Besides incorporating state-of-the-art in segmentation algorithms, this work employs image analysis in a highly usable user interface, to increase the automation of examination. Furthermore, it provides the capability of temporal image registration to avail comparisons of patient status in initial and follow-up examinations.

III. The proposed system

The proposed system avails image analysis methods for vessel representation and measurement and provides diagnostic tools based on these methods. A graphical user interface (GUI) integrates them in a way useful to clinical practice, including visualization and inspection of vessel representations, as well as, the ability to edit them, in order for the healthcare professional to compensate for potential errors of image analysis or ambiguous vessel imaging.

A. Vessel Representation

Specific vessel representation is provided by the binary segmentation image, obtained by the method in [10]. To achieve system modularity, a CORBA-based Interface Definition Language (IDL) is used to invoke the segmentation method. This way, the segmentation method can be updated as state-of-the-art evolves. Also, alternative methods can be invoked for images that are acquired by different modalities (i.e. fluoroangiography).

At a more abstract level, lies the skeletonization of vessels, by which vessels are represented through their medial axes. The skeletonized segmentation image captures the geometry of vasculature, such as the vessel "stem", end-points, junction-points, and vessel overlaps. This skeleton is treated as a topological graph which exhibits mainly tree structure, but includes some circles as some vessels may overlap. Bifurcation points are discovered, through the degree of nodes being 3 and vessel overlaps are characterized by a degree of 4. An IDL-based invocation of the method enables its future upgrade. Measurement of vessel widths is performed as in [10], once for each skeleton point, associating the corresponding measurement to it.

Retinal anatomy is considered by detection of the optical disk. Vessel measurements are assessed with respect to their distance to the optical center, a property of diagnostic significance (see Sec. C). We have enhanced the Mean-Shift

[3] based method in [10], by requiring that the optical disk contains the brightest image region, thus avoiding local minima during optimization. Also, initializing optimization in the vicinity of this region reduces convergence time.

In this work, several pixel-based operations employed by segmentation and skeletonization (i.e. convolution) were re-implemented in the CUDA programming language to parallelize and accelerate their execution. Indicatively, an image of 3000×3000 pixels is processed in $\approx 0.4\,sec$, from tens of seconds required in [10].

Once representations are available they are stored in system files. An XML-indexed file structure is maintained to organize the files of all patients, as each patient may be subject to several examinations, and a GUI component assists the user to find, gather, and sort patient examinations.

B. Visual Inspection and Editing

Inspection and editing of vessel representations is availed through a GUI. This interface includes conventional tools, by which the user can observe image details. The magnification (zoom) function is accompanied with a navigation panel (see Fig. 3) which shows the image thumbnail and enables fast access to different image locations, by clicking on pertinent locations on the thumbnail. Superimposition of representations on the image facilitates their inspection. In addition, brightness/contrast adjustment controls facilitate the inspection of faintly imaged vessels. Most importantly, the interface includes tools enabling interactive measurements and, also, avails the ability to compensate for segmentation errors as image segmentation.

To ease vessel measurement, a variety of selection tools assist the user to select the vessels of interest. The pertinent tools access the obtained representations and, in particular, the graph that represents the skeleton of the vasculature. All selection operations are performed using the mouse device. The simplest case is to select a vessel point, which is considered as the closest skeleton point (or graph node) indicated by the user. To select a vessel segment, two skeleton points are indicated by the user. All possible paths between these two points are recursively found and the shortest one is considered as the result.

The AVR metric averages widths of multiple vessels, at a range of distances $[d_1, d_2]$ from optical center. To achieve the selection, skeleton points at distance d_1 are found. Then, graph paths are recursively grown at the direction away from the disk center, with the recursion ending when distance d_2 is reached. Duplicate paths that may be selected, due to branching points, are thereafter discarded. Finally, paths are sorted in a clockwise order around the optical disk to provide intuitive enumeration in the GUI.

Measurements can be exported in multiple ways. An exhaustive output yields vessel widths per skeleton point, organized in the selected entities. Furthermore, cumulative or per vessel mean average, variance and median of widths can be exported, organized in a spreadsheet format.

The GUI also enables the editing of the extracted representations. The purpose of this component is twofold: (1) provide a way to correct segmentation or skeletonization errors and, thereby, improve measurement accuracy and (2) acquire ground truth results, to be able to compare the accuracy of different segmentation and skeletonization algorithms. The segmentation result can be edited by adding and deleting pixels of the segmentation image, much like in drawing applications, using size-configurable, pencil and eraser tools, as well as, region growing tools. The GUI facilitates editing by enabling zoom in details, storing intermediate results, multiple-level undo, etc. While the segmentation is edited, the skeleton representation and width measurements are automatically recomputed, for the new segmentation. Fig. 2, illustrates the process, for two cases of segmentation errors. In the top row, segmentation underestimates the spatial extent of a faintly imaged vessel (leftmost two images, show initial segmentation and skeleton). By editing the segmentation with a region growing tool the error is recovered (rightmost two images). In the bottom row, two overlapping vessels yield an ambiguous segmentation result, spuriously merging the two vessels into one (left: original image segment, middle: segmentation result). User intervention disambiguates the result into separate vessels (right) providing a more accurate representation and, in turn, AVR estimation. Other representations are simpler to edit, such as the optical disk which can be moved and scaled.

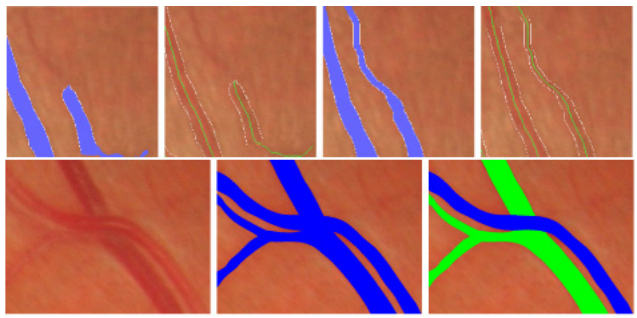

Fig. 2 Editing segmentation results automatically corrects skeletonization (see text).

C. Diagnostic Tools

Calculation of the ratio of Central Retinal Arterial Equivalent (CRAE) over Central Retinal Venous Equivalent (CRVE) is a diagnostic metric for the assessment of hypertensive

retinopathy [13]. Its calculation is available through the proposed system. Its value is determined by the mean widths of arteries and veins within a region of interest which, in turn, requires the classification of the accounted vessels into veins or arteries. This classification is provided by the user through a user interface component that facilitates the process.

Registration of retinal images enables the comparison of vessel width between the initial and follow-up examinations at the level of individual vessels, because it provides the spatial correspondence of the pertinent representations and measurements. Fig. 1 (right) shows a GUI component where images are displayed registered and transparently overlapped for a more extensive comparison. Fig. 3 illustrates the indication of corresponding anatomical points in two images acquired at separate examinations. The user can navigate easily in the magnification through the navigation panels, which appear on the bottom right of each UI panel. (in this figure we have, additionally, superimposed minifications of the entire images above these navigation panels, for better reference).

The proposed system achieved retinal image registration similarly to [9], which registers retinal images as 3D curved surfaces. However, to cope with tissue change, the whole retinal texture is compared and only coarse scale features are considered by the cost function of the matching process. Registration provides a pixelwise mapping between the two images and, thus, in the interface the user indicates a point of measurement in one image and the system provides the corresponding measurement at the other.

Fig. 3 Retinal image registration (see text).

IV. Clinical Study

Data derived from studies conducted in pre-hypertensive patients and in healthy volunteers with a family history of hypertension show that the above changes in microcirculation might precede the development of hypertension and be partially responsible for the establishment of hypertension as well [8]. At the same time, an abundance of data suggests that aortic stiffness is a subclinical index of atherosclerosis [23], associated, independently of other known risk factors, with increased incidence of hypertension [5] and cardiovascular and total morbidity and mortality [20]. Although there is evidence that aortic stiffness is related with microangiopathy in organs such as the brain and kidneys [11], as well as that hypertensive retinopathy is associated with other markers of hypertensive target-organ damage, such as microalbuminuria, renal impairment and left ventricular hypertrophy [16], data on the relationship between arterial stiffness and retinal vascular calibers, remains scarce. The aim of this study was to use the above mentioned software to evaluate for the first time the relationship between aortic stiffness (estimated by augmentation index) and retinal arteriolar narrowing (estimated by retinal vessel diameter), in a naive (with no other comorbidities), except for high blood pressure, adult population and in healthy subjects.

A. Methods

Consecutive hypertensive patients attending the Hypertension Unit of the 2nd Propaedeutic Department of Internal Medicine, Aristotle University, Thessaloniki, Greece were included in the study. The normotensive group was recruited from the Internal Medicine Outpatient Clinic from adults admitted for regular check-up. Procedures in the study protocol were performed according to institutional guidelines and the principles of the Helsinki declaration and were approved by the Ethics Committee of our University. All participants gave written informed consent.

According to the research protocol all participants underwent clinical examination, recording of demographic and anthropometric characteristics and collection of fasting blood samples to determine values of serum lipids. Blood pressure (BP) was measured with oscillometric technique (Omron device 705IT), using standard methodology, after 15 minutes of rest in a seated position. Hypertension was defined as BP $\geq$ 140/90 mmHg. Microcirculation assessment was based on retinal vessels diameter analysis, from retinal photographs obtained by a non mydriatic digital fundus camera (NIDEK AFC-230/210) and analyzed with the software thoroughly described above. Macrocirculation, and specifically arterial stiffness, was estimated using the augmentation index (AI) corrected for the heart rate (AI75) and obtained from the radial artery pressure waveform via applanation tonometry (Sphygmocor device). Augmentation index was defined as the difference between the second and the first systolic peak (P2-P1) expressed as a percentage of the pulse pressure (PP).

Statistical analysis was performed with the Statistical Package for Social Sciences (SPSS) 19. Student t test or Mann Whitney test was used to estimate differences between

Table 1 Baseline characteristics of the study population

	Total (n=105)	Hypertensives (n=70)	Normotensives (n=35)	p value
Age, years	45.5 ± 10.8	45.5 ± 11.1	45.5 ± 10.4	0.792
Sex (Male%)	67.6	77.1	46.9	0.003
Body Mass Index, Kg/m^2	27.1 ± 4.1	27.4 ± 4.1	26.4 ± 4.1	0.186
Height	174.5 ± 9.7	175.2 ± 9.7	172.81 ± 9.61	0.254
Smoking (yes %)	38.1	41.4	31.3	0.326
Systolic blood pressure, mmHg	140.3 ± 18.6	149.2 ± 14.1	120.1 ± 9.2	< 0.001
Diastolic blood pressure, mmHg	89.4 ± 11.8	94.74 ± 8.8	77.13 ± 8.2	< 0.001
Augmentation Index 75%	22.05 ± 12.4	23.62 ± 11.1	19.9 ± 14.8	0.002
Central retinal arteriolar equivalent (μm)	89.4 ± 10.9	87.2 ± 10.5	94.3 ± 10.5	0.032
Central retinal venular equivalent (μm)	119.3 ± 15.5	120.2 ± 16.1	117.1 ± 13.9	0.352
ArterioVenus Ratio	0.757 ± 0.109	0.733 ± 0.106	0.811 ± 0.099	< 0.001
Low Density Lipoproteins	133.4 ± 40.3	139.04 ± 40.1	120.81 ± 38.5	0.036

mean values. Comparison of frequencies was performed by Pearson chi square test. Multivariate linear regression analysis was used to explore the relationship between retinal vascular calibers and AI, while controlling for other covariates. A probability value of $p \leq 0.05$ was considered statistically significant.

B. Results

In total, 105 individuals, aged 18 to 68 years old, participated in the study, 70 of them being hypertensives and 35 healthy controls. Baseline demographic and clinical characteristics of the study population are depicted in Table 1. As expected, hypertensives had statistically significant higher systolic and diastolic BP, higher LDL levels, as well as signs of hypertensive retinopathy, such as narrower retinal arteries and a lower AVR. Linear regression analyses (adjusted R square=0.466 , R square=0.525, p¡0.001) revealed that augmentation index was significantly associated with age (Unstandardized Coefficient (UC): 0.42), p¡0.001), sex (UC:5.35, p=0.041), smoking (UC:-3.78, p=0.048), height (UC:-0.11, p=0.017), diastolic BP (UC: 0.291, p=0.015) and all retinal parameters, CRAE (UC:-1.16, p=0.026), CRVE (UC:1.16, p=0.026) and AVR (UC:-152.2, p=0.015), independently of other factors (weight (UC:-0.35, p=0.080), systolic BP (UC:0.003, p=0.964) and LDL (UC:0.004, p=0.872)).

V. Conclusions

To the best of our knowledge, this is the first study that uses automated retinal vessel evaluation software to assess the relationship between quantitative retinal vascular signs and augmentation index (AI) in an adult, otherwise healthy, hypertensive and normotensive population. The results of the study showed that hypertensive patients exhibit increased arterial stiffness, estimated by AI, and have higher rates of mild hypertensive retinopathy, compared to normotensives. Retinopathy affected mainly the arteries, as CRAE and AVR but not CRVE differed significantly between the two groups. These results are in agreement with data derived from large epidemiological and cross sectional studies [16, 21, 18]. However, the most important finding of this study is the statistically significant linear correlation, independently of age, BMI, smoking, LDL and blood pressure levels between AI and the diameter of the retinal vascular calibers, in a naive population with no other known diseases, except for high blood pressure. Future studies should focus on the clinical significance of this association in the field of cardiovascular disease.

In the course of conducting this study, several conclusions were drawn regarding the usability of the proposed software in the context of performing clinical studies. Some of them have already been taken into account from the formative evaluation of early prototypes of this work [10], while others are planned for future work. In this context, the most useful features of the software were found to be the following.

Improved processing speed enabled conservation of user time and enabled the analysis of images during the patient examination. As images could be processed on the fly, healthcare professionals were not required to plan ahead for this analysis, facilitating the inclusion of the examination in the clinical workflow. In this examination, automation of vessel selection tasks was found to be important again, due to user time conservation. The selection of vessels around the optical disk, also enables the automatic application of measurement protocols. Finally, organized output of vessel measurements in a spreadsheet increased the automation by which statistics over multiple patients were computed.

Regarding the GUI, contrast adjustments, were found useful so that the user can inspect vessels easier and evaluate the extracted representations. Zoom and, in particular, the navigation panel accelerate inspection and editing of

segmentation errors, while keyboard shortcuts and toolbar icons contributed to the ergonomy of interaction.

A future extension targets the increment of segmentation accuracy, as this would directly reduce user interaction and relax the requirement for user expertise. Despite that the employed algorithm is competitive on benchmark datasets [10] we are pursuing further research. Future work also includes the automatic classification of vessels into veins and arteries, as it still requires user expertise.

The conclusion is that without the employed software it would not have been possible to accurately conduct the reported study, as measuring the vessels manually would not only have been immensely time-consuming but would, also, have been subjective and prone to human error. The ability to register images acquired at different time instances enables a next, follow-up study which will avail information of the reversal of symptoms after patient treatment.

ACKNOWLEDGMENTS

This work was supported by the FORTH-ICS internal RTD Programme "Ambient Intelligence and Smart Environments".

REFERENCES

[1] M. Abramoff et al. Evaluation of a system for automatic detection of diabetic retinopathy from color fundus photographs in a large population of patients with diabetes. *Diabetes Care*, 31(2):193–198, 2008.

[2] M. Abramoff et al. Retinal imaging and image analysis. *Biomedical Engineering, IEEE Reviews in*, 3:169–208, 2010.

[3] Y. Cheng. Mean shift, mode seeking, and clustering. *PAMI*, 17(8):790–799, 1995.

[4] B. Dahlof. Cardiovascular disease risk factors: Epidemiology and risk assessment. *American Journal of Cardiology*, 105(1):3–9, 2010.

[5] J. Dernellis and M. Panaretou. Aortic stiffness is an independent predictor of progression to hypertension in nonhypertensive subjects. *Hypertension*, 45(3):426–431, 2005.

[6] N. El-Bendary et al. ARIAS: Automated retinal image analysis system. In *Soft Computing Models in Industrial and Environmental Applications*, pages 67–76, 2011.

[7] A. Grosso et al. Hypertensive retinopathy revisited: some answers, more questions. *British Journal of Ophthalmology*, 89(12):1646–1654, 2005.

[8] M. Ikram et al. Retinal vessel diameters and risk of hypertension: the Rotterdam study. *Hypertension*, 47(2):189–194, 2006.

[9] Y. Lin and G. Medioni. Retinal image registration from 2D to 3D. In *CVPR*, 2008.

[10] G. Manikis, V. Sakkalis, X. Zabulis, P. Karamaounas, A. Triantafyllou, S. Douma, C. Zamboulis, and K. Marias. An image analysis framework for the early assessment of hypertensive retinopathy signs. In *IEEE International Conference on e-Health and Bioengineering*, 2011.

[11] M. O' Rourke and M. Safar. Relationship between aortic stiffening and microvascular disease in brain and kidney: cause and logic of therapy. *Hypertension*, 46(1):200–204, 2005.

[12] M. Ortega et al. SIRIUS: A web-based system for retinal image analysis. *I. J. Medical Informatics*, 79(10):722–732, 2010.

[13] J. Parr and G. Spears. Mathematic relationships between the width of a retinal artery and the widths of its branches. *American Journal of Ophthalmology*, 77(4):478–483, 1974.

[14] T. Sairenchi et al. Mild retinopathy is a risk factor for cardiovascular mortality in Japanese with and without hypertension: the Ibaraki prefectural health study. *Circulation*, 124(23):2502–11, 2011.

[15] H. Struijker-Boudier et al. Evaluation of the microcirculation in hypertension and cardiovascular disease. *European Heart Journal*, 28(23):2834–2840, 2007.

[16] C. Sun et al. Retinal vascular caliber: systemic, environmental, and genetic associations. *Survey of Ophthalmology*, 54(1):74–95, 2009.

[17] S. Thom et al. Differential effects of antihypertensive treatment on the retinal microcirculation: An anglo-scandinavian cardiac outcomes trial substudy. *Hypertension*, 54(2):405– 408, 2009.

[18] A. Triantafyllou, M. Doumas, P. Anyfanti, E. Gkaliagkousi, X. Zabulis, K. Petidis, E. Gavriilaki, P. Karamaounas, V. Gkolias, A. Pyrpasopoulou, A. Haidich, C. Zamboulis, and S. Douma. Divergent retinal vascular abnormalities in normotensive persons and patients with never-treated, masked, white coat hypertension. *American Journal of Hypertension*, 2013.

[19] C. Tsai et al. Automated retinal image analysis over the internet. *IEEE Transactions on Information Technology in Biomedicine*, 12(4):480–487, 07 2008.

[20] C. Vlachopoulos et al. Prediction of cardiovascular events and all-cause mortality with arterial stiffness: a systematic review and meta-analysis. *Journal of the American College of Cardiology*, 55(13):1318–1327, 2010.

[21] T. Wong and R. McIntosh. Systemic associations of retinal microvascular signs: a review of recent population-based studies. *Ophthalmic Physiological Optics*, 25(3):195–204, 2005.

[22] T. Wong and P. Mitchell. Hypertensive retinopathy. *New England Journal of Medicine*, 351(22):2310–2317, 2004.

[23] S. Zieman et al. Mechanisms, pathophysiology, and therapy of arterial stiffness. *Arteriosclerosis, Thrombosis, and Vascular Biology*, 25(5):932–943, 2005.